12-31-1993

Investigation of Dislocations in GaAs Using Cathodoluminescence in the Scanning Electron Microscope

K. L. Pey
National University of Singapore

J. C. H. Phang
National University of Singapore

D. S. H. Chan
National University of Singapore

Recommended Citation

Utah State University
MERRILL-CAZIER LIBRARY

INVESTIGATION OF DISLOCATIONS IN GaAs USING
CATHODOLUMINESCENCE IN THE SCANNING ELECTRON MICROSCOPE

KL Pey[#], JCH Phang, DSH Chan[*]

Centre for Integrated Circuit Failure Analysis and Reliability
Faculty of Engineering, National University of Singapore
10 Kent Ridge Crescent, Singapore 0511
Republic of Singapore

Abstract

Electrically active dislocations in Si-doped {100} GaAs substrates were observed using the cathodoluminescence (CL) technique in the scanning electron microscope (SEM). CL contrast profiles were experimentally obtained from the dislocations at different beam energies. Based on the CL model for localized defects in semiconductors developed earlier by Pey, the depths of the dislocations were found by locating the beam energy at which maximum CL contrast occurred. A preferential etching technique for {100} GaAs was employed to reveal the dislocations and to measure their depths. The etched depths obtained were compared to the predicted results from the theoretical model developed. The discrepancies in the results were attributed to a Cottrell atmosphere of point defects around the dislocation core.

[#]Present address:
Institute of Microelectronics
Block 750E, Chai Chee Road, #07-03/04
Chai Chee Industrial Park, Singapore 1646
Phone No. : (65)249-7593
Fax No. : (65)449-6158

[*]Address for correspondence:
DSH Chan, Department of Electrical Engineering
National University of Singapore
10 Kent Ridge Crescent, Singapore 0511
Phone No. : (65)772-2132
Fax No. : (65)779-1103

Introduction

Cathodoluminescence, electron beam induced current (EBIC) and spatially resolved photoluminescence (PL) have been recognized as powerful techniques for the characterisation of electrically active defects, particularly dislocations, in opto-electronic materials. Among these techniques, CL is the only method that is contactless and has a spatial resolution of 1 μm or less. Hence, it is important in the assessment of materials for opto-electronic devices. A theoretical study of the information depth of CL signal on homogeneous semiconductor materials has been described by Hergert and Pasemann (1984). Both CL and CL/EBIC techniques have been applied to defect study by Löhnert and Kubalek (1984), Jakubowicz et al. (1987), Brummer and Schreiber (1972), Brummer and Schreiber (1974), Bode et al. (1988) and Czyżewski and Joy (1990). Other workers such as Böhm and Fischer (1979) and Rasul and Davidson (1977) have measured a reduction in the minority-carrier lifetime in the dislocation vicinity using PL and CL respectively. It is suspected that in most of these studies that the impurities or point defects or impurity-complex atmosphere are changed around the dislocation core. Very recently, Schreiber and Hildebrandt (1991), Schreiber and Hergert (1989), Schreiber et al. (1991) and Hildebrandt et al. (1989) used the combined EBIC and CL technique to investigate the depth and recombination strength of individual dislocations in crystalline semiconductors. The interpretation of the experiments was performed by using a unified theoretical description of CL and EBIC matrix signals including the defect contrasts. Eckstein et al. (1989, 1989a) also used the combined EBIC/CL technique to study the role of impurity aggregation and defect decoration on the recombination behaviour of dislocations in GaAs. They observed an increase in signal contrast and changes in the contrast profiles. The observed results were interpreted as a homogeneous decoration of dislocations, the formation of precipitates at the dislocations and a reduced minority-carrier diffusion length in the bulk.

In this paper, dislocations in GaAs were studied and analysed using the CL technique. The experimental set-up employed for collecting linescan profiles across dislocations lying parallel to the top surface in {100} Si-doped GaAs substrates is described. The CL contrast profiles from the dislocations at different beam energies under stress free
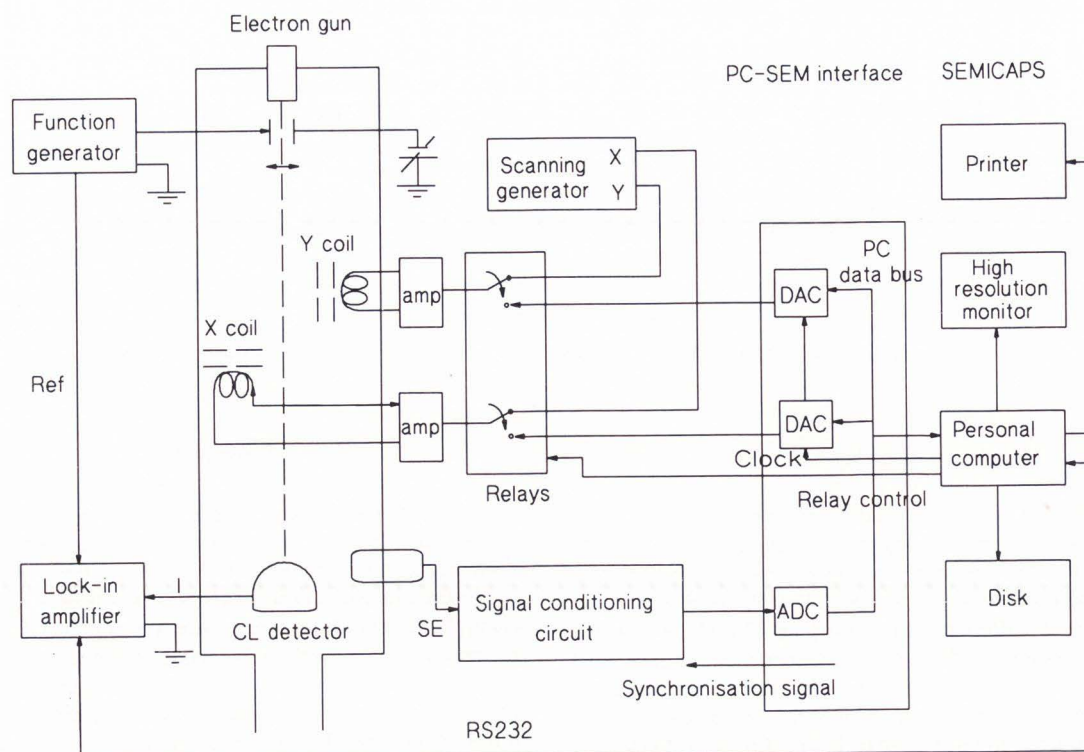
Fig. 1. Schematic diagram of the instrumentation.

conditions were experimentally obtained. Using the CL model for localized defects in semiconductors described by Pey *et al.* (1993), the depth of the dislocations was found by locating the beam energy at which maximum CL contrast occurred. A preferential etching technique for {100} GaAs (Weyher and van de Ven 1983 and 1986, Weyher and van Enckevort 1983) was used to reveal the dislocations and to measure their depths. The etched depths obtained were compared to the measured results from the theoretical model. The discrepancies in the results are attributed to a Cottrell atmosphere of point defects around the dislocation core.

Measurement of Dislocation Contrast Profiles

Instrument set-up

The schematic diagram of the instrument set-up is given in Fig. 1. The scanning electron microscope (SEM) used in this study was a Philips 505. Computer control of the main SEM parameters was achieved by a scanning electron microscope image capturing and processing system (SEMICAPS) developed in our laboratory. In this set-up, SEMICAPS was mainly used to control the beam scanning of the SEM.

As the CL signal levels were very weak, the signal-to-noise ratio was enhanced by using lock-in amplification with synchronized electron beam blanking. The beam blanking system was supplied by the SEM manufacturer and the lock-in amplifier was a SR530 dual phase lock-in amplifier from Stanford Research Systems. The chopping action was accomplished by blanking the primary electron beam with parallel plates below the anode of the SEM. The use of the lock-in amplifier instead of the standard amplifier resulted in higher sensitivity. The integration time of the lock-in amplifier was made small so as to obtain a resolution of 512 data points per line. Typical line scan times varied from 200 seconds up to 300 seconds depending on the number of samples collected per data point required.

A solid-state detector was used to detect the CL emissions. The photo-sensitive diodes were operated with zero biasing. The integral CL signals were fed directly into the current input of the lock-in amplifier with a gain of 10^6V/A. The data was collected by the SEMICAPS microcomputer reading from the RS232 interface of the lock-in amplifier. Preprocessing of the raw data (averaging) and programming of the measurement procedure (lock-in amplifier) were carried out by the SEMICAPS microcomputer.

All the CL measurements were performed at room temperature. The primary electron beam current and voltage were carefully monitored during the course of the experiments to ensure compliance with low level injection conditions (Pankove 1971).

Software description

The SEMICAPS microcomputer, which controlled the entire system, was an IBM PC 386 compatible. The programs for this work could be divided into two parts. Part I comprised programs to record linescans and to store the data. Part II consisted of programs to analyse the stored linescans offline. Fig. 2 illustrates the basic concept of the core programs (Part I) to record the linescans. After initialisation, all the required information such as the number of samples and the output file

name was fed into the microcomputer. This was performed interactively. The next step was to define the marker region and trace the linescan across the defect of interest. For the definition of the marker region, a field of arbitrary size was selected and a prominent feature of this field was "marked" as the reference throughout the entire CL experiment. For the trace of the linescan, it was defined by moving the cursor on the SEM video screen to the desired position through SEMICAPS. After programming the lock-in amplifier to the appropriate range, the programs continued automatically, depending on the specified parameters. The programs of Part II were basically used to perform the CL contrast calculation and to plot the contrast profiles.

Results of measurements

The samples used in this study were cleaved from Si-doped GaAs crystals grown with the Hybrid Bridgman techniques with carrier concentration of $8.2\text{-}14 \times 10^{17}$ cm^{-3} and {100} orientation of the surfaces. The etched pit density for this set of samples was 100-200cm^{-2}.

Fig. 3(a) shows the CL micrograph of a dislocation in a 300 μm thick GaAs substrate. The geometrical arrangement of this defect is shown in Fig. 3(b). Linescans with normally incident electron beam were recorded along the trace marked in Fig. 3(b). This line is perpendicular to the electrically active dislocation. It will be shown that this dislocation going in <110> direction is located at a certain depth parallel to the surface.

Fig. 4(a) and (b) show the measured CL contrasts and the corresponding $C(E)$ versus beam energy plots. CL contrast is defined as $(I_{CL(t,E)}-I_{CL(\infty,E)})/I_{CL(\infty,E)}$, where $I_{CL(\infty,E)}$ and $I_{CL(t,E)}$ are the CL intensities from the material far away from any defect and at a distance t from the centre of the defect of interest respectively, $C(E)$ is the CL contrast at the centre of the defect i.e. t = 0 and the E in the parenthesis denotes the value of the beam energy. From the results, for 7.5 keV < E < 12 keV, the magnitude of $C(E)$ increases. At 12 keV, the magnitude of $C(E)$ reaches its maximum $C(E)_{max}$, and for E > 12 keV, the magnitude of $C(E)$ decreases with E. The "contrast reversal" of this particular dislocation occurred at about beam energy $E_{max} = 12$ keV (Fig. 4(b)). This set of experimental data points have shown good qualitative correlation with the simulation results shown in Pey et al. (1993) for subsurface localized defects. It was shown there that in the variation of $C(E)$ at different beam energies, the energy at which maximum contrast occurs depends on the depth of the defect and is independent of the defect strength and size. The plot of $C(E)$ versus beam energy and defect depth from Pey et al. (1993) is reproduced in Fig. 5. Based on the technique proposed in Pey et al. (1993), the depth of the dislocation was measured by substituting $E_{max} = 12$ keV into the plot relating the depth of defect d to the beam energy at which $C(E)_{max}$ occurs and the
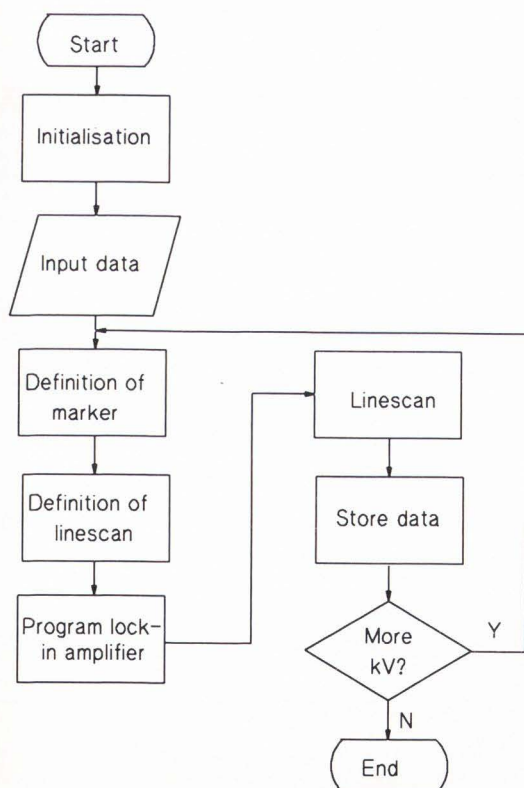

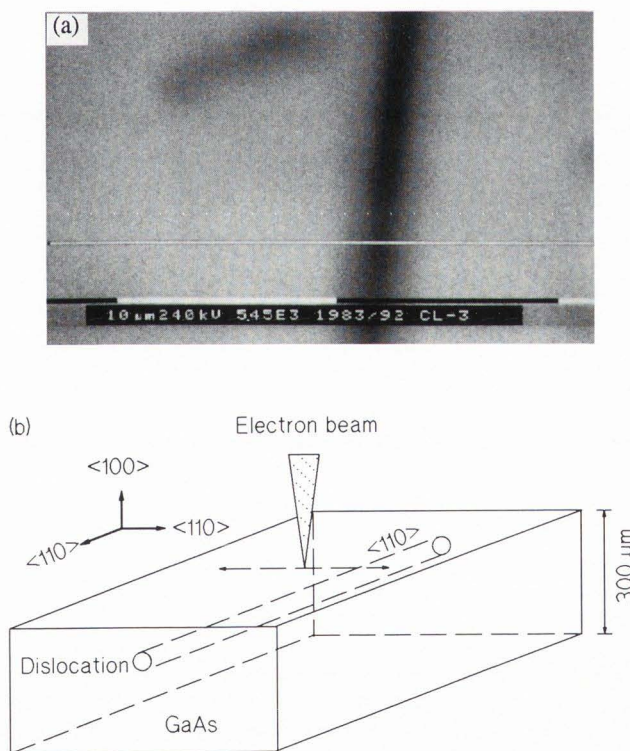Fig. 2. Flow chart of the programs used to collect and store linescan data.

Fig. 3. (a) CL micrograph of a dislocation (No. 1) in a GaAs substrate (b) geometrical arrangement of the defect. The horizontal line shown in (a) represents the trace where the linescans were performed for defect analysis.
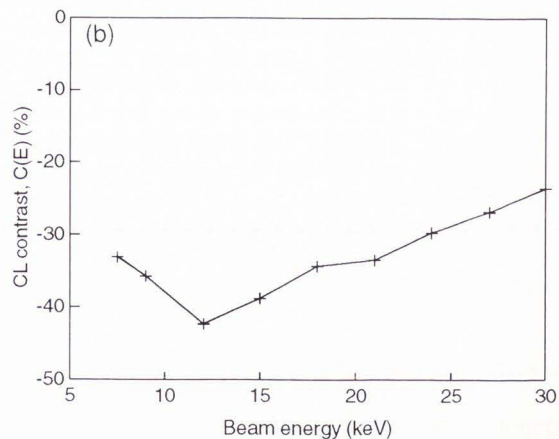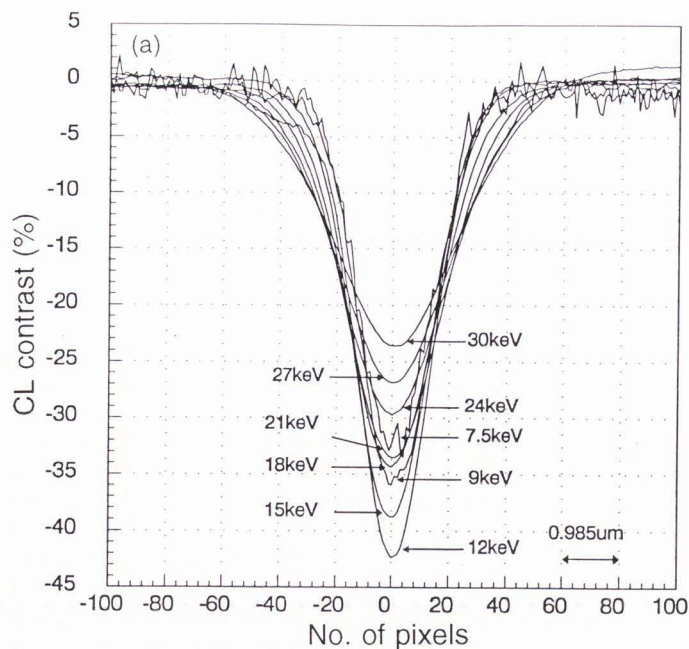
Fig. 4. (a) CL contrast profiles collected along the horizontal line shown in Fig. 3(a) for dislocation No. 1. (b) $C(E)$ versus E plot reveals that the contrast reversal occurred at 12 keV for dislocation No. 1.

value was found to be 0.66 μm.

Figs. 6(a), (b) and (c), and Figs. 7(a), (b) and (c) show the results of dislocations collected from two other {100} GaAs substrates. The geometrical structures were similar to that of Fig. 3(b) except that the defects were oriented in a <100> crystallographic direction, and the beam was scanning along a <100> direction which was perpendicular to the dislocations. The "contrast reversal" for these two defects occurred at 6 keV and 9 keV respectively. Again using the same method described, these were found to correspond to a depth of 0.26 μm and 0.43 μm respectively. From the $C(E)$ versus beam energy plots, it is interesting to observe that the magnitude of the maximum contrast can vary from 22% for dislocation No. 2 in Fig. 6(a) through 42% for dislocation No. 1 in Fig. 3(a) and to about 90% for dislocation No. 3 in Fig. 7(a).

Verification of Defect Locations

A selective etching method was used to reveal and confirm the defects investigated by the CL method. The etch rate of CrO_3-HF-H_2O mixtures on n-type Si-doped {100} GaAs crystals is well documented and known to be a function of etch composition (Weyher and van de Ven 1983). The CrO_3-HF aqueous solutions were therefore used for this purpose.

Experimental procedure

The etching solutions were prepared by diluting basic HF/CrO_3 mixtures. The notation $D_{1:x}S_{a/b}$ for this etchant has been adopted from Weyher and van de Ven (1983):

$D_{1:x}$ - dilution of 1 volume part of basic mixture with x volume parts of water; and

$S_{a/b}$ - basic mixture consisting of a and b volume parts of HF (48 wt%) and CrO_3 (33 wt%) aqueous solutions respectively.
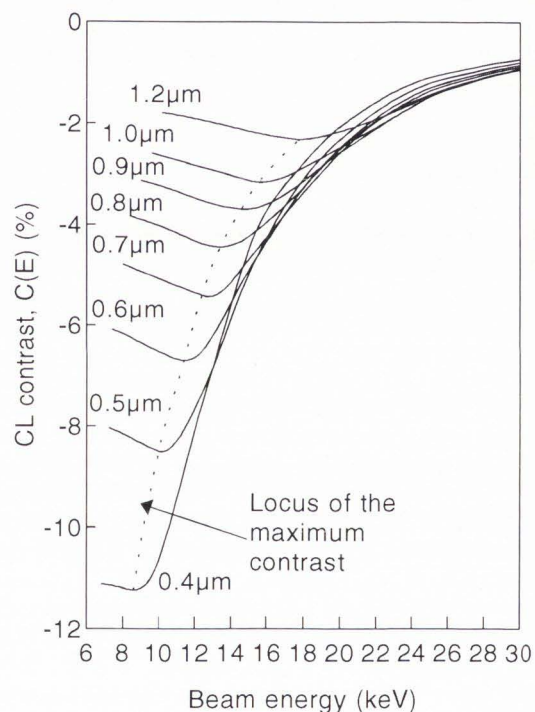

Fig. 5. $C(E)$ profiles for point defects located at different depths.

All the samples investigated by the CL technique were chemically cleaned with trichloroethylene, acetone and methanol for 15 minutes each. The residual oxide layer protecting the surfaces of the samples from dust contamination was removed with a HCl-water solution just before each etching experiment.
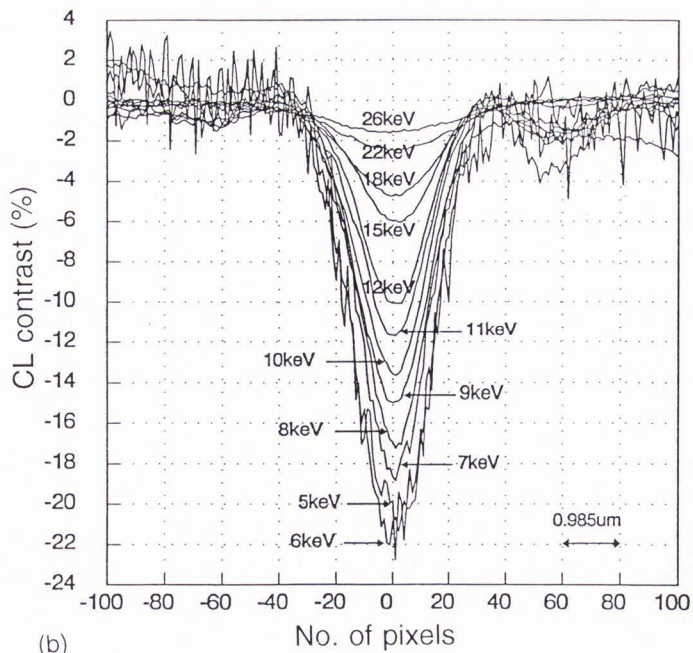
Fig. 6. (a) CL micrograph of a <100> dislocation (No. 2) in a {100} GaAs substrate. The horizontal line represents the trace where the linescans were performed for defect analysis. (b) CL contrast profiles collected along the horizontal line shown in (a). (c) **C**(E) versus E plot reveals that the contrast reversal occurred at 6 keV for dislocation No. 2.

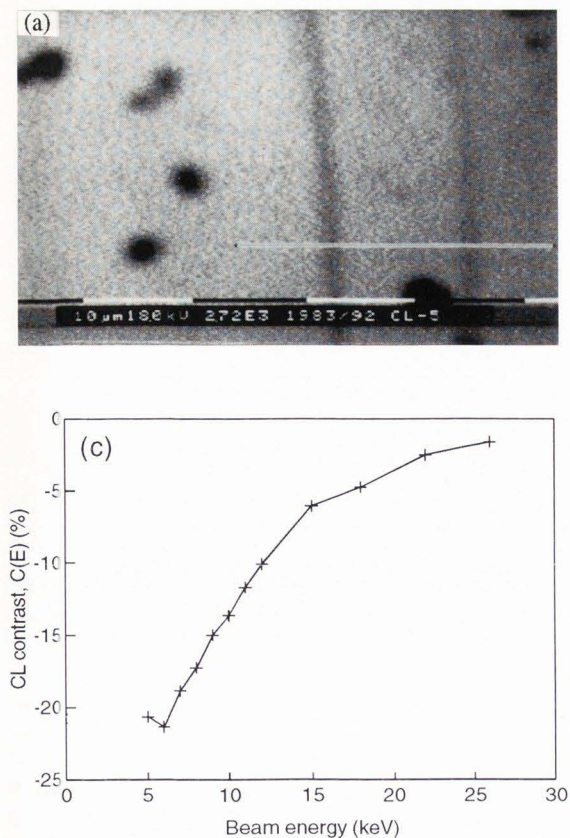**Fig. 7.** (a) CL micrograph of a <100> dislocation (No. 3) in a {100} GaAs substrate. The horizontal line represents the trace where the linescans were performed for defect analysis. (b) CL contrast profiles collected along the horizontal line shown in (a). (c) **C**(E) versus E plot reveals that the contrast reversal occurred at 9 keV for dislocation No. 3.
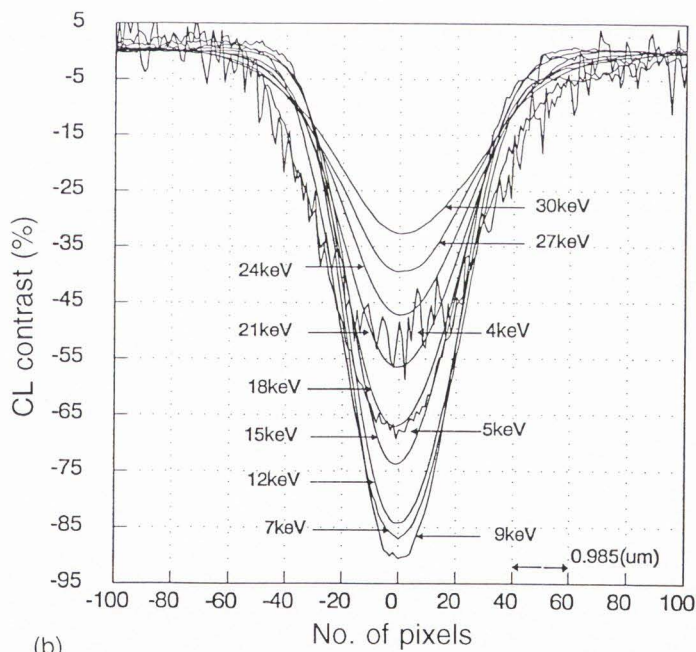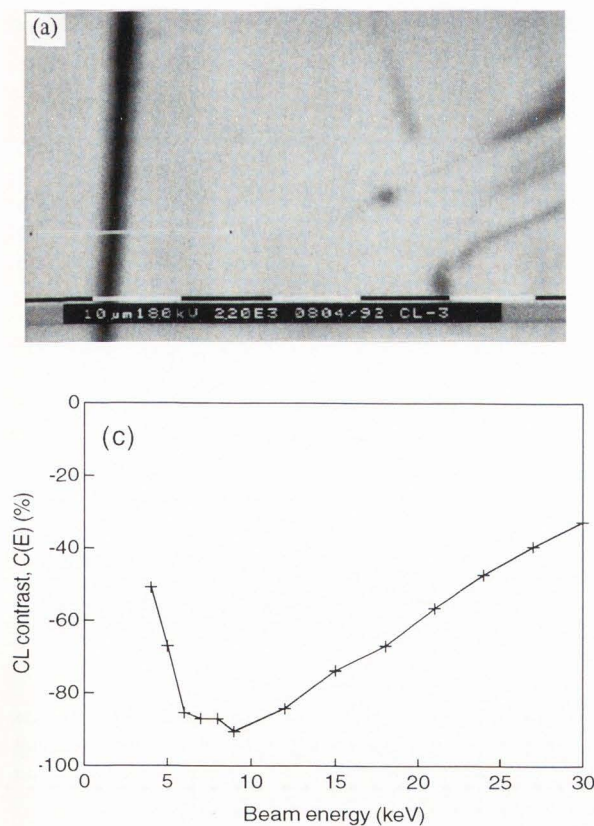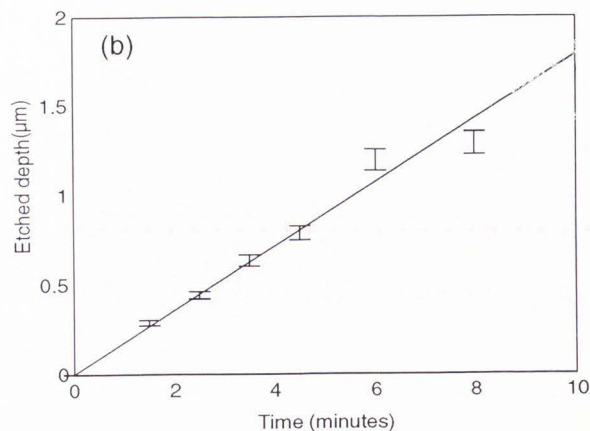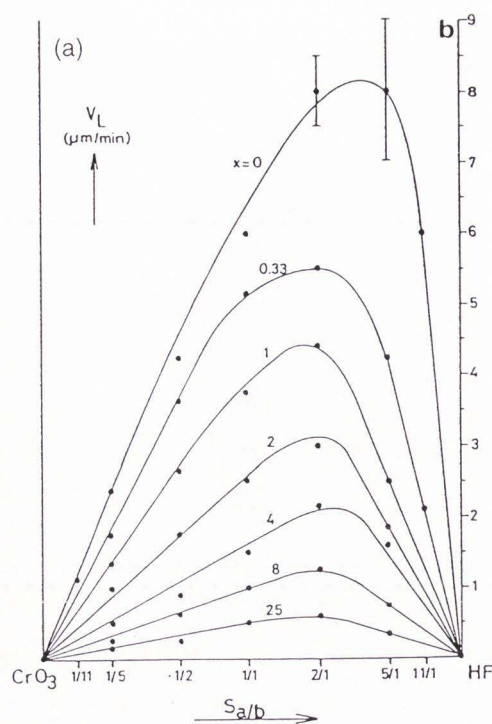
Fig. 8. (a) Etch rate of {100} Si-doped GaAs as a function of basic mixtures ($S_{a/b}$ containing a and b volume parts of 48 wt% HF and 33 wt% CrO_3 in H_2O, respectively) for different ratios ($D_{1:x}$) with illumination (Weyher and van de Ven 1983). (b) The calibrated etching rate of the experimental system (x = 4 and a:b = 1:2) used in the present study.

The samples were etched without stirring in a Teflon beaker at 20°±2°C. The thickness of the solution layer above the sample surface was constant in all the etching experiments. A control sample cleaved from the same wafer was partially masked with photoresist to enable the exact measurements of the etched depth by an Alpha Step 200 surface profiler from Tencor Instruments. After each successive etching, the surface features were examined with a SEM until the desired feature corresponding to the dislocation of interest appeared.

Etch rates and surface morphology after etching

The etch rates under illumination reported in Weyher and van de Ven (1983) are reproduced as shown in Fig. 8(a). The error of this method was about ±5%. For the present work, the value of x and the ratio of a:b were 4 and 1:2 respectively. This range of values gave a slow etching rate which enabled better control to be exercised. In addition, a yellow light source was employed to improve the resolution of the etch figures. Fig. 8(b) shows the calibrated etching rate for the present system at temperature of about 20.5°C. The action of this etchant is illustrated by the micrographs in Figs. 9(a) and (b). The CL micrograph shown in Fig. 9(a) gives the commonly observed dislocations and other non-radiative defects. Fig. 9(b) is the secondary electron (SE) image of the corresponding area after removal of about 2.4 μm which reveals one to one correspondence of the non-radiative regions in Fig. 9(a). Different defects can be distinguished with well resolved etch patterns. These etch figures are mainly etch hillock or ridges (Weyher and van de Ven 1986).
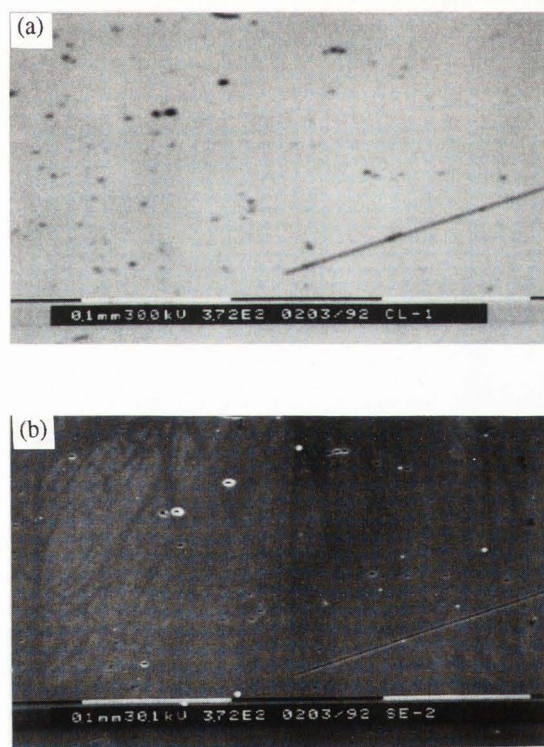

Fig. 9. (a) CL micrograph of a Si-doped GaAs substrate showing non-radiative contrasts. (b) SE micrograph revealing the defects of the area in (a) after removal of a layer of about 2.4 μm from the top surface.

Results

Fig. 10(a), (b) and (c) reveal the etch features seen using the SE mode of the SEM of the corresponding dislocations shown in Figs. 3(a), 6(a) and 7(a) respectively. The depths at which the respective dislocations first appeared after etching were 0.38 µm, 0.09 µm and 0.17 µm. The results are also tabulated in Table 1. These showed that the defects observed using the CL mode were subsurface localized dislocations. A typical step profile of the control sample of dislocation No. 1 shown in Fig. 3(a) is illustrated in Fig. 11.

Discussion

Comparing the results of the selective etching experiments and the dislocation depths predicted by the simulation model, it can be observed that for a given dislocation, the theoretical depth is always greater than the etched depth P_d. The difference varies from 0.17 µm for dislocation No. 2 to 0.28 µm for dislocation No. 1. These discrepancies can be explained as follows. It has been widely accepted that dislocations can be treated as charged lines surrounded by an electric field (Jakubowicz 1986) and/or additional defects surrounding the geometrical dislocation core (Kaufmann *et al.* 1987). Therefore, the modelling of the dislocation has to take into account a cylinder of finite width (Löhnert and Kubalek 1984, Jakubowicz 1986, Kaufmann *et al.* 1987), which is represented by Wd in Pey *et al.* (1993). In this model, Wd can be further interpreted as an environment in which the dislocation is evenly and homogeneously decorated by impurities, point-defects or impurity complex (Eckstein *et al.* 1989, 1989a) and characterized by a reduced non-radiative carrier lifetime (Böhm and Fischer 1979).

Fig. 12 shows a scheme of a hypothetical density distribution of photocarriers around a grown-in dislocation of D-1 type in Weyher and van de Ven (1986). According to van de Ven *et al.* (1986), the photoetch rate of n-type GaAs in CrO_3-HF solutions depends on the number of photogenerated carriers which are available for the depassivation and
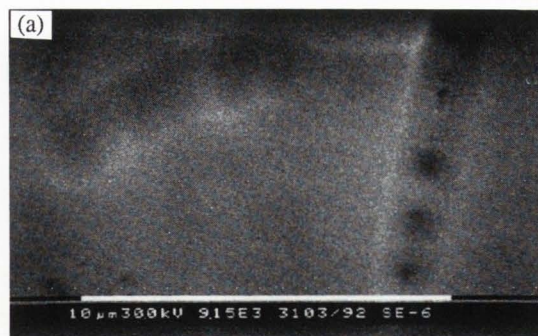
Fig. 10 (right). SE micrographs revealing the defects after the selective etching of (a) dislocation No. 1 in Fig. 3(a), (b) dislocation No. 2 in Fig. 6(a) and (c) dislocation No. 3 in Fig. 7(a).

Table 1 Summary of parameters of the dislocations in the GaAs samples.

Dislocation no.	Orientation	$C(E)_{max}$ (%)	E_{max} (keV)	Predicted depth, **d** (µm)	Etched depth, P_d (µm)	Difference in depth (µm)
1	<110>	42	12	0.66	0.38	0.28
2	<100>	22	6	0.26	0.09	0.17
3	<100>	90	9	0.43	0.17	0.26

Fig. 11. A step profile in the controlled sample used to measure the etched depth of dislocation No. 1.

Fig. 12. Scheme proposed in Weyher and van de Ven (1986) for D-1 type dislocation etch-hillock formed during photoetching : (a) cross-sectional view (b) the corresponding hypothetical photocarrier distribution. d_0 = diameter of the core of dislocation; d_1 = diameter of cylindrical region depleted in photocarriers (I_0) due to efficient recombination at the dislocation core; D = diameter of the impurities (Cottrell) atmosphere with less severely (in comparison with the core region) reduced amount of photocarriers (I_1), i.e. 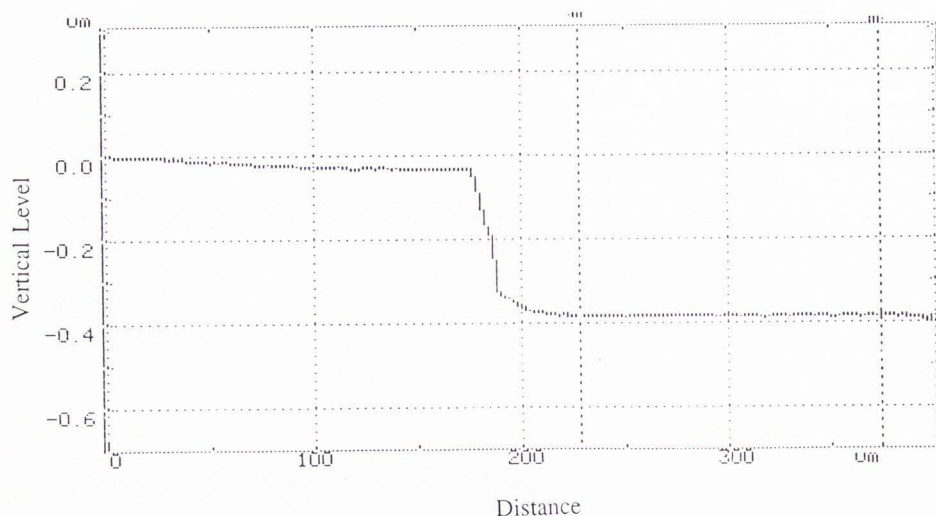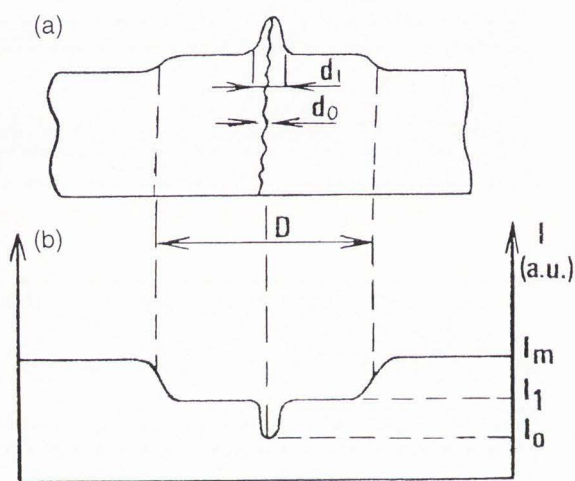increased recombination rate; I_m = average density of photocarriers in dislocation-free matrix (bulk) of GaAs crystal.

dissolution reactions. Effective recombination of these carriers, which may occur both at levels introduced by lattice disturbances around a dislocation (e.g. deformation field) and at levels introduced by impurities in the Cottrell atmosphere, which correspond to d_1 and D in Fig. 12, consequently leads to a lower net photo effect. In addition, Weyher and van de Ven

(1986) commented that the photoetching of CrO_3-HF solution is particularly sensitive to very small variations of electrically active impurities around the dislocation and therefore, the amount of photocarriers I_1 is smaller than that (I_m) of the bulk and an etch feature corresponding to the presence of a Cottrell atmosphere is often obtained.

Extending the Weyher and van de Ven model to horizontal dislocations, a hypothetical model of photocarrier distribution is postulated as shown in Fig. 13. In this figure, d is measured from the centre of the core to the surface. P_d is the photoetched depth determined by the etching experiment. Wd, interpreted as the size of the Cottrell atmosphere is, therefore used to account for the difference between d and P_d. Based on this model, Wd in the three samples was 0.28 µm, 0.17 µm and 0.26 µm. These values represent the extent of the Cottrell environment around the dislocations of interest.

Conclusions

Dislocation depths in Si-doped {100} GaAs crystals grown by the Hybrid Bridgman method have been measured from the experimental CL contrast profiles using the algorithm described by Pey et al. (1993). A contrast reversal was observed for each set of results, which agreed qualitatively with the theoretical predictions for subsurface localized defects. The selective photoetching method used was found to be a useful tool in identifying and verifying the defect location. From the experimental results, it is believed that the differences between the measured depths and the etched depths of the subsurface dislocations are due to the influence of the Cottrell atmosphere containing point defects around the dislocation core. Thus the extent of the influence of the dislocations can be estimated by calculating the difference in depths.
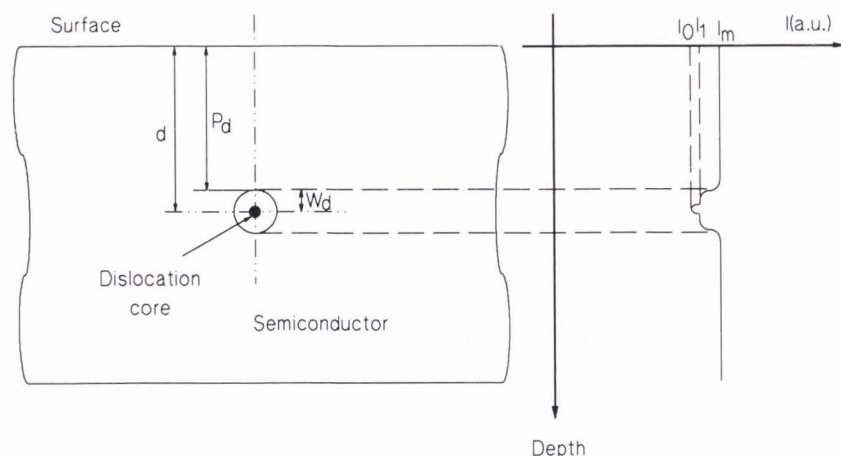
Acknowledgements

Fig. 13. A hypothetical model for a horizontal dislocation etch-hillock formed during photoetching of a $\{100\}$ surface in GaAs. d = depth of dislocation measured from the top surface to the centre of the core; Wd = radius of the Cottrell atmosphere shown in Fig. 12; P_d = Photoetched depth determined by the etching experiment.

References

Bode M, Jakubowicz A and Habermeier H-U (1988) A computerized signal acquisition system for the quantitative evaluation of EBIC and CL data in a SEM. Scanning **10**, 169-176.

Böhm K and Fischer B (1979) Photoluminescence at dislocations in GaAs and InP. J. Appl. Phys. **50**, 5453-5460.

Brummer O and Schreiber J (1972) SEM CL studies of grain boundaries in CdS. Ann. der Physik **28**, 105-107.

Brummer O and Schreiber J (1974) The CL contrast of dislocations in CdS. Kristall und Technik **9**, 817-829.

Czyżewski Z and Joy DC (1990) Monte Carlo simulation of CL and EBIC contrasts for isolated dislocations. Scanning **12**, 5-12.

Eckstein M, Jakubowicz A, Bode M and Habermeier H-U (1989) Impurity aggregation at individual dislocations in GaAs observed by means of a simultaneous electron beam induced current and cathodoluminescence technique. Appl. Phys. Lett. **54**, 2659-2661.

Eckstein M, Jakubowicz A, Bode M and Habermeier H-U (1989a) Investigation of gettering behaviour of dislocations in GaAs by simultaneous EBIC/CL measurements. In: Microscopy of Semiconducting Materials 1989, Conf. Series. Inst. Phys., Bristol, 755-760.

Hergert W and Pasemann L (1984) Theoretical study of the information depth of the cathodoluminescence signal in semiconductor materials. Phys. Stat. Sol. **a85**, 641-648.

Hildebrandt S, Hergert W and Schreiber J (1989) Theoretical investigation of combined CL and EBIC measurements on crystal defects, In: Int. Symp. on Struct. Prop. Disloc. Semicond. 1989, Conf. Series No. 104. Inst. Phys., Bristol, 221-226.

Jakubowicz A (1986) Theory of cathodoluminescence contrast from localized defects in semiconductors. J. Appl. Phys. **59**, 2205-2209.

Jakubowicz A, Bode M and Habermeier H-U (1987) Simultaneous EBIC/CL investigations of dislocations in GaAs. In: Microscopy of Semiconducting Materials 1987, Conf. Series. Inst. Phys., Bristol, 763-768.

Kaufmann K, Kisielowski-Kemmerich C, Heister E and Alexander H (1987) EBIC - Investigation of fresh and grown in (immobile) dislocations in GaAs. In: Defect Recognition and Image Processing in III-V Compounds II, ed. ER Weber, Elsevier Science Publisher BV, Amsterdam, 163-170.

Löhnert K and Kubalek E (1984) The cathodoluminescence contrast formation of localized non-radiative defects in semiconductors. Phys. Stat. Sol. **a83**, 307-314.

Pankove 1971 In *Solid State Physical Electronics Series*, Prentice-Hall, New Jersey, 1971, pp. 242-257.

Pey KL, Chan DSH and Phang JCH (1993) A numerical method for simulating cathodoluminescence contrast from localized defects. In: Microscopy of Semiconducting Materials 1993. Conf. Series. Inst. Phys., Bristol, in press.

Rasul A and Davidson SM (1977) SEM measurements of minority carrier lifetimes at dislocations in GaP, employing photon counting. Scanning Electron Microsc. 1977;I: 233-240.

Schreiber J and Hergert W (1989) Combined application of SEM-CL and SEM-EBIC for the investigation of compound semiconductors, In: Int. Symp. on Struct. Prop. Disloc. Semicond. 1989, Conf. Series No. 104. Inst. Phys., Bristol, 97-107.

Schreiber J, Hergert W and Hildebrandt (1991) Combined application of SEM-CL and SEM-EBIC for the investigation of compound semiconductors. Appl. Surf. Sci. **50**, 181-185.

Schreiber J and Hildebrandt S (1991) Quantitative evaluation of recombination activity of dislocations by combined SEM-CL/EBIC. J. de Phys. Colloque C6, C6-15 - C6-19.

van de Ven J, Weyher JL, van den Meerakker JEAM and Kelly JJ (1986) Kinetics and morphology of GaAs etching in aqueous CRO_3-HF solutions. J. Electrochem. Soc. **133**, 799-806.

Weyher JL and van de Ven J (1983) A selective etching and photoetching of $\{100\}$ Gallium Arsenide in CRO_3-HF aqueous solutions I. Influence of composition on etching

behaviours. J. Crystal Growth **63**, 285-291.

Weyher JL and van de Ven J (1986) A selective etching and photoetching of {100} Gallium Arsenide in CRO_3-HF aqueous solutions III. Interpretation of defect-related etch figures. J. Crystal Growth **78**, 191-217.

Weyher JL and van Enckevort WJP (1983) A selective etching and photoetching of {100} Gallium Arsenide in CRO_3-HF aqueous solutions II. The nature of etch hillocks. J. Crystal Growth **63**, 292-298.

Discussion with Reviewers

L.J. Balk: Photoluminescence (W. Heinke and H.J. Queisser, "Photoluminescence at dislocation in GaAs", Phys. Rev. Lett., 1974 33, 1082-1084) and cathodoluminescence (L.J. Balk *et al.*, "Investigation of As-grown dislocations in GaAs single crystals in the SEM", SEM Part I, 1976, 257-264) were carried out already earlier. How does your work correlate with these papers, how do the results compare?

Authors: The PL and CL results previously reported showed that there is a continuous decrease of Se concentrations towards the core for as-grown dislocations in GaAs. The main purpose of this work is to demonstrate a method that is capable of determining the depth of a subsurface defect using the CL technique. Since the chemical etching method used is extremely sensitive to the presence of a Cottrell atmosphere around dislocations, the method was further explored to estimate the extent of the influence of the Cottrell atmosphere. Hence, the only correlation between the presence and previous work is that the results are explained by the presence of stable a Cottrell atmosphere.

L.J. Balk: Why do think that CL yields a significantly better spatial resolution than PL, especially taking into account the carrier diffusion preceding the recombination process?

Authors: Both CL and PL involve carrier generation, diffusion and recombination. The main difference which affects the spatial resolution of the methods would be the size of the excitation source. We believe that a finely focused electron beam is superior. Recent applications of CL to the studies of optoelectronic semiconducting materials have shown that the spatial resolution ranging from a few hundred nanometres down to 60nm (Warwick 1991, Wada *et al.* 1988) is attainable.

L.J. Balk: What do you believe the Cottrell atmosphere is like? It is associated with segregation of dopant, is the dopant there still in the same manner electronically active as it is in the undistributed bulk material or is it forming clusters or similar structures?

Authors: We believe that the Cottrell atmosphere, i.e. impurity atmosphere, is a region where there is an accumulation of impurities. The formation of a Cottrell atmosphere around a dislocation is due to the migration of impurity atoms in the crystal to the dislocation under the attractive influence of their respective strain fields. If the concentration of the impurities lies below their solid solubilities, they are distributed along the dislocations. However, if the impurity concentration exceeds the equilibrium solid solubility, precipitation at discrete nucleation sites along the dislocation takes place (Rhodes 1964). Patel (1956) has shown that the binding between the dislocations and the impurity atoms in Ge is not entirely caused by their elastic interaction, but also by chemical or electronic bonding.

L.J. Balk: What is the advantage of a solid state detector compared to a photomultiplier, especially considering signal/noise ratio problem?

Authors: The solid state detector offers several advantages over conventional photomultiplier tube systems for photon collection: ease and simplicity of implementation, low cost, high collection efficiency and wide spectral range. The solid state detector used in this work is a set of PIN Si photodiodes with low dark current characteristics. However, a photomultiplier tube does have better signal/noise characteristics than a solid-state detector.

L.J. Balk: How did you identify dose structures in CL micrographs (Fig. 9) to be dislocations and not other features and how did you identify the nature of the dislocations itself other than just by etching techniques. An unequivocal identification could be gained either by X-ray topography experiments (Balk *et al.*, "Analysis of crystal depths in GaAs by use of X-ray topography and scanning electron microscopy", BEDO, 1975 8.) or by time-resolved CL techniques (M. Hastenrath and E. Kubalek, "Time-resolved cathodoluminescence in scanning electron microscopy", SEM part I, 1982, 157-173). The double dot structures in Fig. 9 could well be loops of as-grown dislocations.

Authors: Apart from the microscopic CL and etching analysis, we did not use other techniques to determine the type of crystalline defects and their nature. However, it has been reported in the literature by many workers (Yacobi and Holt 1990) that dislocations in the CL mode appear as dots when viewed end on (e.g. threading dislocations) or as lines (e.g. misfit dislocations). Weyher and van de Ven (1983), Weyher and van de Ven (1986) and Weyher and van Enckevort (1983) have also given a good description on the different kinds of dislocation-related etch figures. We agree that the double dot structures in Fig. 9 could correspond to loops of as-grown dislocations.

L.J. Balk: Can you give any numbers on the accuracy of both theoretical discrimination of the contrast maximum and of the experimental data.

A. Jakubowicz: The paper says that CL and etching give different results for the dislocation depths, which is due to the presence of Cottrell atmospheres of point defects. The differences are around 0.2 up to 0.3 μm. This suggests that both techniques allow the authors determining the position of dislocations in bulk material with an accuracy better than 0.2 μm. Could the authors comment on how various theoretical and experimental factors/parameters affect the accuracy of their CL method of determination of dislocation depths?

Authors: The simulation model that was used to generate the theoretical results uses a finite difference scheme to calculate the distribution of excess minority carriers. The accuracy of the model is predominantly determined by discretisation errors. An error of 3.8% or less is attainable. The experimental error for discriminating the maximum contrast in this work was found to be ±13% for dislocation No. 1, ±12% for dislocation No. 2 and -17% to 8% for dislocation No. 3.

J.F Bresse: It is not clear from the work mentioned in the reference Pey *et al.* (1993) that the energy at which the maximum in the signal occurs is independent on the defect size. Can you give more explanation of this fact?

Authors: The CL contrast of a defect is basically determined by the amount of carriers available for radiative recombination, which in turn is determined by the defect properties and the depth dose function of the electron beam. It has been found that, regardless of the defect size, the maximum amount of the interaction between the defect and generated carriers always occurs at a specific beam energy which corresponds to E_{max}. Since the defect centre is assumed to be at the same location even for different sizes, E_{max} should occur at the same beam energy although the magnitude of the contrast can vary significantly.

J.F Bresse: Can you give a more precise explanation for the difference of depth observed by the CL measurements and the etching method. It seems that the strong contrast observed for the three dislocations correlate with the fact that a Cottrell atmosphere is present.

Authors: Our simulation results have shown that even for a point defect i.e. defect with zero dimension, the contrast profile can be very broad and its full-width-half-maximum can be as large as 2μm depending upon the values of the defect parameters. Hence, the dislocation CL contrast observed should not just involve a Cottrell atmosphere, but also dislocation core effects. Weyher and van de Ven (1986) have shown that the etching method is very sensitive to the very small variations of electrically active impurities around dislocations. The method has been used to reveal the extent of the influence of a Cottrell atmosphere around grown-in dislocations. We think that apart from the experimental errors, Cottrell atmosphere around the dislocations is the best explanation to account for the difference in depths observed.

J.F Bresse: Starting from the contrast values, can you give a more precise estimation of Wd?

Authors: We have developed an algorithm to determine the value of Wd based purely on the CL contrast versus image resolution plots. It is expected that this approach will offer better accuracy since it does not require the etching method. The work has been submitted for publication.

S. Myhajlenko: Would the authors mention the chopping frequency used and if applicable, the frequency range investigated in the dislocation-contrast experiments. Did the

authors observe any dependence of the contrast on frequency, such as those reported in a related study by A. Ourmazd *et al.* (1981) "Measurement of contrast from individual dislocations by lock-in EBIC", Inst. Phys. Conf. Ser. No. 61, 519-520 (Bristol Series).

Authors: In most of the experiments, the frequency used for the lock-in circuit was fixed at 20 Hz. However, we have performed calibration for our system for the frequency range 5 Hz to 5 kHz and did not observe any significant variation in the signals.

S. Myhajlenko: Would the authors expect any significant effect from (dislocation) strain on (i) the dislocation depth-contrast behaviour, and (ii) the discrepancy between the etching experiments and theory. I refer to the fact that different dislocation types have different strain components.

Authors: The exact effect of the different inherent structures of dislocation on CL contrast is unclear. A parameter called defect strength has been used to characterise the properties of the recombination centres at the dislocations in our simulation model. The defect strength was found to have a significant impact on the magnitude of the dislocation contrast, but not on E_{max}. We are looking into the possibility of incorporating the dislocation strain into the model.

A. Jakubowicz: The authors describe in detail the experimental conditions, but - in my opinion - do not give enough information on their simulation they have done to derive the dislocation depths from CL results. For example, they no not say anything about the values of such parameters as the diffusion length and light absorption coefficient, which they have used in their simulation. If these parameters are not of importance then this should explained in the paper. However, if these parameters do play a role, then - in my opinion - the authors should include these data, and explain why they have chosen these and not other values. This is important because the authors compare qualitatively two different techniques (etching and CL) and draw important conclusions from the observed differences.

Authors: According to our numerical simulation results of Pey *et al.* (1993), no significant variation was observed in E_{max} due to a change in defect strength or defect size for the range of values simulated. For example, when defect depth was 0.8μm, E_{max} was pretty constant at 12.5 keV, despite significant variations in defect size and strength. Although we are still in the midst of simulating the effects of bulk diffusion length, light absorption coefficient and surface recombination velocity on E_{max}, we do not expect a significant effect. These parameters affect the overall CL level but not the beam energy at which $C(E)_{max}$ occurs because this is driven predominantly by the depth-dose function of the electron beam, i.e. the depth at which the depth-dose function is maximum, and this is determined by the beam energy.

Additional Reference

Patel JR (1956) Delay time of plastic flow in Ge. Phys. Rev. **101**, 1436-1437.

Rhodes RG (1964) Imperfections and Active centres in Semiconductors. Pergamon Press, New York, 204-257.

Wada K, Kozen A, Fushimi H and Inoue N (1988) A high resolution cathodoluminescence microscopy utilizing magnetic field. Jap. J. Appl. Phys. **27**, L1952-L1954.

Warwick CA (1991) Developments in high resolution scanning cathodoluminescence microscopy. In: Microscopy of Semiconducting Materials 1991, Conf. series. Inst. Phys., Bristol, 681-688.

Yacobi BG and Holt DB (1990) Cathodoluminescence Microscopy of Inorganic Solids. Plenum Press, New York, 121-164.